

Seismic rehabilitation of masonry structure strengthening by two distinct FRPs

Ataur Rahman

Khulna University of Engineering and Technology, Khulna 9203, Bangladesh

Tamon Ueda

Faculty of Engineering, Hokkaido University, Sapporo 060-8628, Japan

ABSTRACT: Huge losses on both human lives and properties from the recent earthquake in Nepal, demonstrate the need for strengthening of masonry structure due to their poor seismic performance posed by their inherent brittleness and low tensile strength. This paper investigates the in-plane shear performance of externally strengthened masonry walls using two types of fiber reinforced polymer (FRP) sheets, they are- artificial FRPs such as CFRP and PET-FRP which are relatively expensive FRPs have been used in conjunction with low-cost FRPs made from natural fiber such as JUTE and COTTON fiber. An experimental research program was undertaken, in which brick masonry walls were tested for static loading after installing PET-FRP, CFRP, JUTE-FRP and COTTON-FRP sheets on their surface in three different configurations. The results demonstrate that a significant increase in the in-plane shear capacity of masonry can be achieved by bonding those FRP sheets to the surface of the walls.

1 INTRODUCTION

Very recent earthquakes in Nepal have caused an extensive damage in a large number of old masonry buildings. Damage was mainly due to the in-plane shear failure and the out-of-plane bending or slip during the tremor of a 7.9 magnitude earthquake. The majority of those URM buildings have been constructed with little or no attention to seismic considerations. This has resulted in a large inventory of buildings that lack ability to dissipate energy through inelastic deformation during seismic activity. Therefore, there is an urgent need to improve the performance of URM structures by retrofitting and strengthening them to resist potential earthquake damage.

The lateral shear strength of a URM wall depends on the failure mode of the wall, which is governed by a number of variable parameters, such as masonry aspect ratio (L/H), vertical compression on the masonry (σ_n), compressive strength of the masonry (f_{mc}), tensile strength (f_{tu}), shear strength (τ_u), masonry elastic modulus (E_{me}), and masonry shear modulus (G_{me}). These variables control the inelastic mode of failure of masonry shear walls. The lateral strength of masonry shear walls is limited by flexural cracking, rocking followed by toe crushing, diagonal shear cracking, and sliding shear at the bed-joint (see Fig. 1). It should be noted that not all these failure modes will involve collapsing of the masonry shear wall, and the final failure may be a combination of several failure modes. A more general way of representing the various failure modes of masonry shear wall is given by Drysdale and Hamid (2008) as seen in Fig. 2, where the interactions between normal and shear

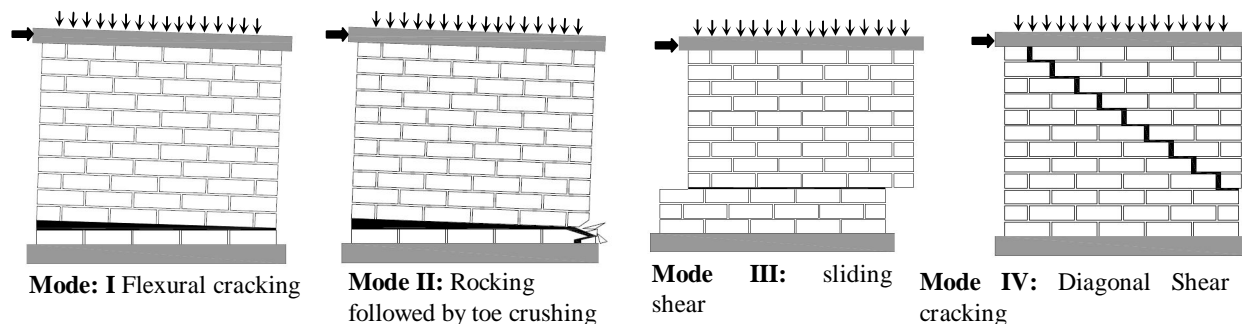


Figure 1. Different Failure modes of URM

stresses on the masonry bed joints are shown. It is evident in Fig. 2 that the modes of failure in masonry shear wall are generally dictated by the magnitude of vertical compression force applied over the wall. However, a rationally developed failure criteria should be able to predict the tensile, compressive and shear types of failure (Zhuge et al. 1998).

Various approaches have previously been undertaken to investigate masonry strengthened with FRPs. There is no harmonized test method available to determine the shear performance of masonry elements under lateral loading (Bosiljkov et al. 2008, Tomazevic and Gams 2009). A TNO report (TNO 2004) gives an exhaustive discussion and literature review of various methods for testing of masonry shear wall, that have been undertaken by different researchers. None of them simulate real-time behavior, but have been chosen because they reproduce static or kinematic boundary conditions, which can be easily interpreted with a perceived analytical model.

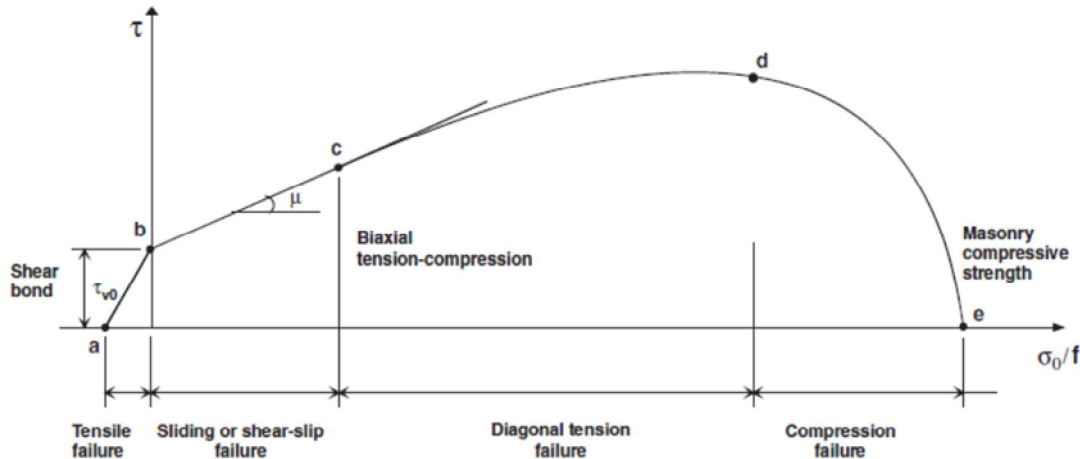


Figure 2. Behavior of URM under combined shear and normal stress (Drysdale et.al. 1994)

The use of FRPs as a shear reinforcing material for RC members is becoming increasingly popular since the early 1990s, due to their various advantages that include low weight to strength ratio, non-corrosiveness, minimum disruption to the use and no significant change in the geometry. The aim of seismic retrofitting is to upgrade the ultimate strength/deformation of the structure by improving the structure's ability to undergo inelastic deformation without fully collapsing during an earthquake. The application of FRPs to URM is one of the methods that attempt to improve integrity during an earthquake event by upgrading the ultimate strength/deformation.

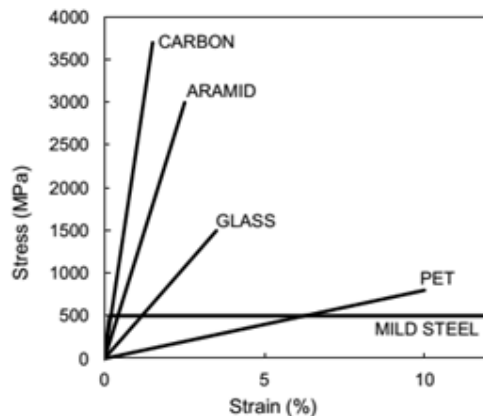


Figure 3. Tensile strength of different FRPs

Externally bonded PET-FRP with a large fracturing strain is a retrofitting technique that has drawn significant attention as a unique alternative to CFRP or GFRP (Fig. 3). This is due to its pronounced failure strain and relatively low material cost, without compromising the other advantages of FRP. The main objective of using FRPs is to enhance performance of a structure at normal loading conditions and to offer greater resistance at the times of severe loading. Neither too much stiffness nor very high strength materials will be coherent with

the overall performance of the masonry structures. It is commonly observed that materials with high strength/stiffness produce very little deformation prior to fracture in tension, if any, will normally be brittle and explosive in nature, which would not be an expected failure mode in a well-designed structure. On the other hand, a highly compliant material with low strength would not be well suited for the purpose of strengthening. Cost of the material is also a major concern during retrofitting works. Artificial FRPs such as CFRP, PET-FRP etc are quite expensive materials for masonry strengthening. On the contrary natural fibers like JUTE and COTTON (see Fig. 4) are relatively low cost materials for the purpose of retrofitting. Locally available materials are always the best option for any kind of structural renovation, which keep the total strengthening cost within the capacity of the local people.

When FRPs are bonded to the surface of the wall, a compressive crushing type of failure is quite common (Hamid et al. 2005; Wang et al. 2006). Also, premature debonding or fracture of FRP was commonly observed during the test and, in general, FRP could not reach its ultimate strength (Ehsani et al. 1997; Stratford et al. 2004; ElGawady et al. 2005). Experimental tests indicate that the failure patterns are affected by the strength, orientation, amount and anchorage length of FRP (Santa-Maria et al. 2006; Alcaino and Santa-Maria 2008; Marcari et al. 2007). In general, the possible failure mode for masonry strengthened with FRP can be a combi-



Figure 4. Common types of fiber sheet

nation of several mechanisms (CNR DT200 R1/2013) such as, excessive cracking due to tensile stresses in the wall, crushing of masonry in the compression zone, shear-slip of masonry, FRP debonding, and FRP rupture.

In this study, PET-FRP and CFRP have been used as artificial but expensive strengthening materials. On the other hand JUTE-FRP and COTTON-FRP have been used as low cost naturally available strengthening materials. A comparison of these two in term of cost and strength has been shown in this study. The strength/stiffness of CFRP is higher than PET-FRP, whereas PET-FRP poses a relatively higher fracturing strain than CFRP. On the contrary, natural fiber like JUTE and COTTON are much weaker than these two, but are quite available at low cost. The purpose of this study is to show the difference in behavior of masonry shear wall strengthened by two distinct FRPs and the superiority of the one type of FRP over the other. Ultimate load bearing capacity, deformation at peak load, and mode of failure, are observed in this study for different arrangements of the FRPs.

2 EXPERIMENTAL PROGRAM

2.1 Specimen details

In this experimental study, a total of 15 masonry panels having a nominal dimensions of $1270 \times 1020 \times 120$ mm, were fabricated. All of the walls were made with single layer running bond of bricks having a dimensions of $240 \times 120 \times 74$ mm with an average compressive strength of 30 MPa. A 10 mm thick mortar joint with a compressive strength of 22 MPa that are commonly seen in masonry construction, was used throughout. Due to the anchorage at the wall top and bottom, the topmost and bottommost layers of the brick were ineffective in transferring the shear. So, the effective height (830 mm) of the wall comprised of the remaining ten courses of brick, offered an aspect ratio (L/H) of 1.45 (Fig. 5 and Fig. 6). In this table, RW stands for Reference Wall, P for PET-FRP, C for CFRP, JT for JUTE-FRP, CT for COTTON-FRP, D for Diagonal strip configuration, G for Grid system, F for Fully wrapped wall and S for Solid bricks.

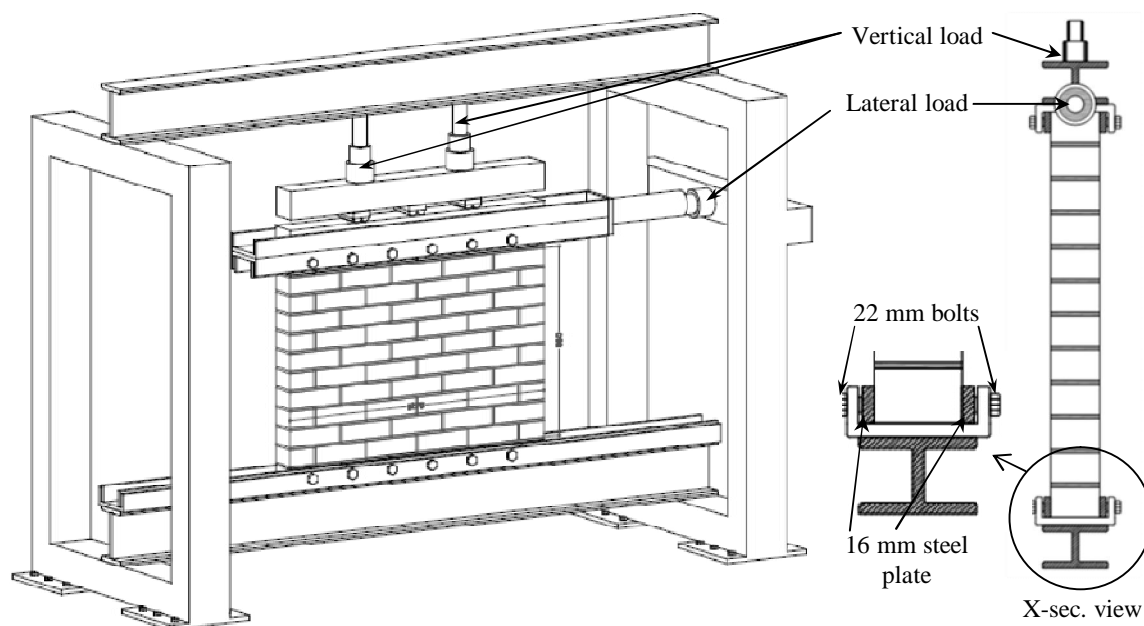


Figure 5. Schematic diagram of experimental setup of shear wall

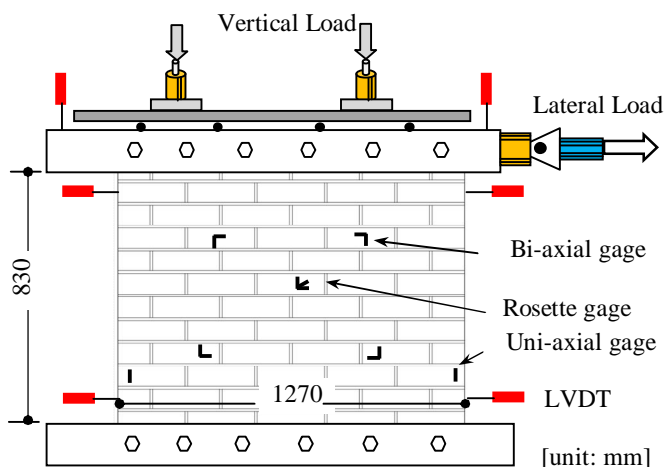


Figure 6. Instrumentation of control wall RWS

2.2 Specimen preparation

FRP sheets having unidirectional fibers, were applied using a wet layup procedure on wall specimens in three different configurations as shown in Fig. 7. At first, the wall specimens were cleaned by removing loose mortar and dirt with the help of a wire brush. Epoxy putty (filler) was used to fill the depression on the wall surface to provide a smooth plane surface ready for FRP laying. A thin layer of primer was then applied all over the wall

to seal the pores in the masonry so that the subsequent application of epoxy resin would not be absorbed. Epoxy resin having the properties indicated in Table 1 was then applied over the wall wherever necessary. Fiber sheets were cut to the length and width needed to cover approximately 20%, 40% and 100% of the wall gross area (see Fig. 7). Resin was then applied with a roller brush all over the sheet strip so that it was fully saturated by the resin. As soon as the application of the resin was completed, the FRP strips were laid over the wall and wrapped tightly to keep them in place. For the diagonal strip, the wall corners were cut in the same dimension width (80 mm) as the strip [see Fig. 7(b)] in order to avoid sharp edges and problem in wrapping.

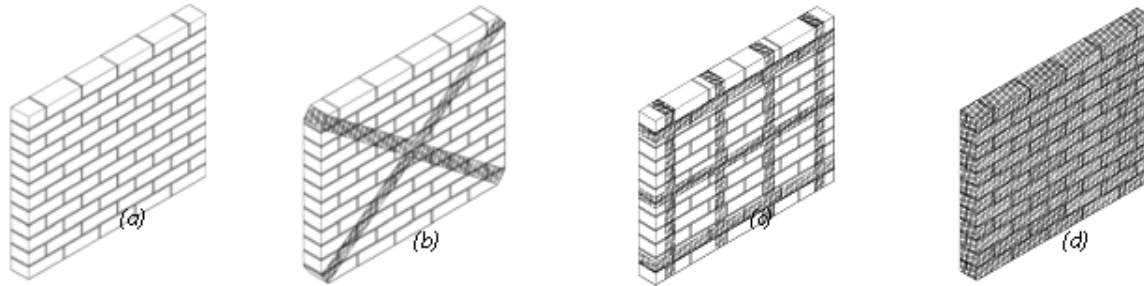


Figure 7. Wrapping technique of masonry wall by FRP, (a) Control wall(RWS); (b) FRP diagonal bracing (CSD, PSD); (c) FRP strips in grid system (CSG, PSG); (d) Fully wrapped by FRP (CSF, PSF)

Table 1. Properties of FRPs and Adhesive

| Properties | FRP materials | | | | Adhesive |
|----------------------------|---------------|---------------------|-------|--------|-------------------|
| | PET (600) | CFRP (FTS-C1-20) | JUTE | COTTON | RESIN (D-90 R) |
| Tensile strength (MPa) | 740 | 3400 | 25 | 19 | 45 |
| Elastic modulus (MPa) | 10000 | 245000 | 107 | 199 | 1.56 |
| Elongation at fracture (%) | 10±1 | 1.5 | 22.7 | 9.8 | 28 |
| Thickness (mm) | 0.841 | 0.111 | 1.304 | 1.298 | - |
| Width (mm) | 300 | 250 | 500 | 750 | - |

2.3 Test setup and FRP anchorage

After the required curing period, the wall was transferred to the testing frame. The wall top and bottom were anchored to the top and bottom channel beams, with the help of twelve 22 mm bolts as shown in Fig. 5. Between the wall and the side of the channel beam, a 16mm thick steel plate was inserted so that pressure could be applied on the wall by tightening the bolts. Gypsum plaster was used to fill a gap between the wall and the steel plate. For FRP strengthened walls, the FRP itself was wrapped in a U-shape anchorage, so there was almost no chance of slippage of the FRP during the experiment. Although this kind of anchorage system is not very much practical for the real structure, it has been chosen for this experimentation to avoid premature anchorage failure of FRP prior to attaining full shear strength. A pre-compression of 38 kN which is equivalent to uniform pressure of 0.25MPa, was applied on the top of the wall through two hydraulic jacks, prior to the shear loading to simulate the load of the structural component coming on the wall from above in the real structure. These two vertical loads restricted the rotation of the top beam only to some extent, as the beam was not restrained against rotation during the evolution of lateral load.

2.4 Instrumentation and Data Acquisition

Sufficient uni-axial, bi-axial and rosette strain gages, LVDTs, and load cells (50 tons capacity) were used to record all the necessary information during the testing. A lateral load was applied in a pull-out manner by a 50-ton capacity center-hole jack, with a remote pump, until the complete failure of the masonry wall. A universal coupling-joint was used to minimize the effect of bending due to rotation of the top beam during the evolution of loading. All of the data (displacement, strain, and load) were recorded through a digital data logger. Fig. 6 shows the instrumentation of a typical shear wall.

Table 2. FRP Configuration for Masonry Specimens

| Wall ID | FRP(%) | Peak Load, kN | Def. at Peak Load, mm | FRP configuration |
|---------|--------|---------------|-----------------------|-------------------|
| RWS1 | – | 48 | 8.7 | -- |
| RWS2 | | 30 | 5.4 | |
| PSD1 | 20 | 114 | 8.9 | Diagonal |
| PSD2 | | 101 | 24.7 | |
| PSG1 | 40 | 129 | 10 | Grid |
| PSG2 | | 88 | 9.7 | |
| PSF1 | 100 | 111 | 6.9 | Full |
| PSF2 | | 168 | 6.5 | |
| CSD1 | 20 | 95 | 2.9 | Diagonal |
| CSD2 | | 94 | 4.4 | |
| CSG1 | 40 | 134 | 2.5 | Grid |
| CSG2 | | 99 | 7.0 | |
| CSF1 | 100 | 107 | 2.7 | Full |
| JTSF | 100 | 104 | 21.4 | Full |
| CTSF | 100 | 133 | 15.7 | Full |

3 EXPERIMENTAL OBSERVATION

3.1 Observation of crack pattern and load-deformation characteristic

URM wall (RWS1, RWS2)

These reference walls were tested under physical and boundary conditions similar to those of the rest of the walls mentioned in Table 2. In the case of wall RWS1, when the lateral load reached 42 kN, a flexural crack appeared at the heel of the wall, and propagated towards the toe as shown in Fig. 10, and the load dropped slightly. Lateral load was further increased to 45 kN, and the crack opening widened as the crack propagated all the way to the toe of the wall. No crushing was observed at the toe. After the applied load reached its peak, it did not decrease much with the increased displacement, which furthered the shear-slip along the crack plane as shown in Fig. 8. Similar crack pattern was observed on the wall RWS2. When the lateral load reach about 23 kN, a flexural crack appeared on the wall heel as shown in Fig. 8, and the load dropped to 19 kN. Lateral load was further increase to 30 kN, and the crack further propagated almost halfway the length of the wall and took a downturn in a stepped fashion and travelled all the way to the toe of the wall. During this evolution of crack, no significant degradation of load was observed rather the crack opening widened and a faster crushing at the wall toe was observed which caused a rapid decrease in load. This kind of failure in URM wall under shear is reported in a number of papers (Stratford et al. 2004; Salmanpour et al. 2013; Bosiljkov et al. 2003; ElGawady et al. 2007 etc).

The load-deformation characteristics of RWS are given in Fig. 9. It is quite evident from the figure that, before appearance of any potential flexural crack, the load-deformation relationship is quite linear. As the first crack appeared at the wall heel, the load dropped by a little and could still undergo shear deformation with substantial resistance in a manner that can be characterized as elasto-plastic behavior. This post peak behavior may be dependent on the mortar interface shear behavior with residual stress (Rahman and Ueda 2014), which did not diminish with applied displacement. If flexural cracking is followed by toe crushing, a softening in post-peak load is generally observed as in the case of RWS2. So, it can be said that a premature flexural cracks normally followed by either a toe crushing or a sliding shear type of failure. For slender walls, rocking type of failure is usually seen in many experimental shear walls.

Fig. 10 shows the variation of vertical pre-compression with the progress of lateral load. It is evident from Fig. 10 that the vertical load on the far-end increased with the progressive shear, while the vertical load went down on loaded-end. This is due to the fact that, with the increase of lateral load, the top beam on the wall underwent a small rotation, which exerted a vertical upward pressure on the far-end jack on the wall. However,

the average vertical load (broken line in Fig. 10) did not change much from the initial stipulated value of 19 kN.

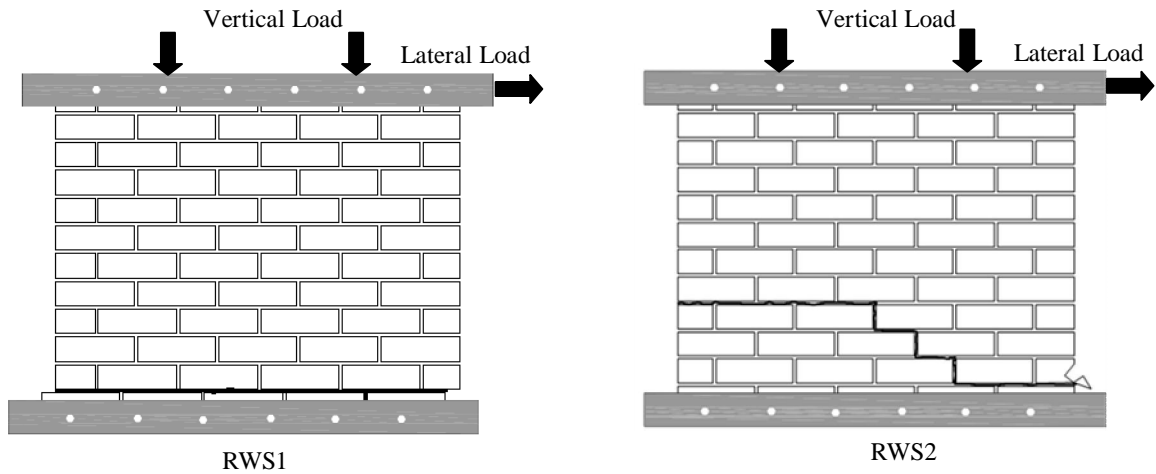


Figure 8. Schematic illustration of crack in RWS

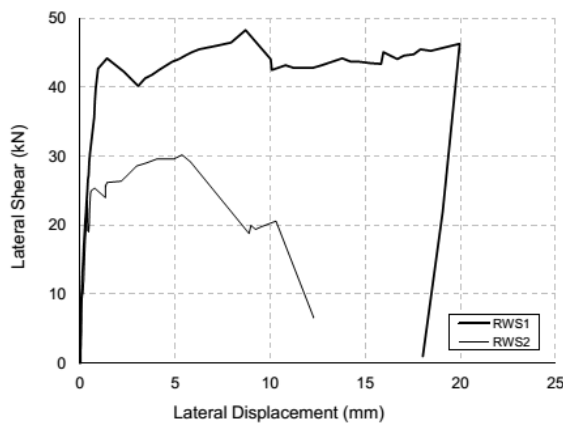


Figure 9. Load-displacement response of RWS

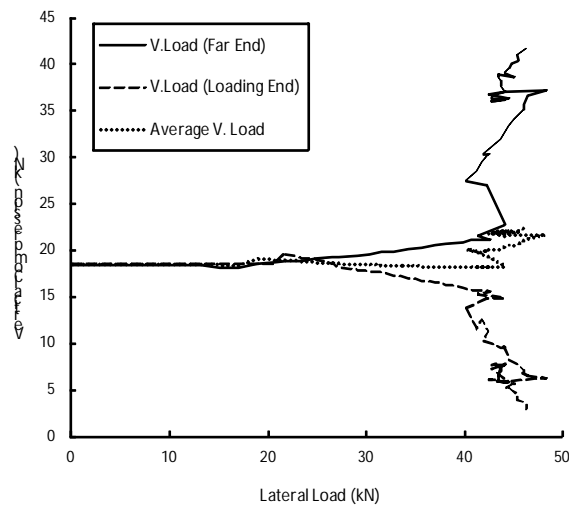


Figure 10. Variation of vertical load with progressive shear

3.2 FRP reinforced walls

Wall with diagonal bracing by FRP strips (CSD, PSD)

These walls were externally reinforced by two diagonal FRP strips each, of 80 mm in width in a fashion shown in Fig. 6(b), which covered approximately 20% of the gross wall surface. In the case of the wall with CFRP strips (CSD1), at a load of 76 kN, two flexural cracks appeared at the wall top on the loading end and at the wall bottom on the far end (see Fig.11) followed by some debonding of the CFRP tension diagonals. No rupture or damage of the CFRP was observed. For wall CSD2, the initially stiffness was similar to that CSD1, but at a load of 75 kN, some fine line cracks appeared at the top of the wall on far end and started to propagate downward in a stepped fashion. Once the load increased to a maximum of 94 kN, a sudden rupture of the diagonal tension strip on the both sides of the wall took place and the load suddenly dropped to the half of the peak load. Accumulated compressive stress caused a complete failure at wall toe just before the rupture of the CFRP strip which can be seen Fig. 11.

In the case of the wall reinforced with PET-FRP strips (PSD1 and PSD2), similar crack patterns were observed on these two walls and they were stepped diagonal shear crack followed by some toe crushing(see Fig. 11). The peak load of 114kN and 101 kN respectively did not attenuated much with the applied displacement for quite a long time, and at that stage the experiment was ceased.

The load-deformation characteristics of all of the FRP reinforced walls are given in Fig. 12. It is obvious in these two figures that the shear capacity of PET-FRP strengthened walls are little higher than their counterpart

of CFRP strengthened walls but the deformation at peak load for the case of PSD is much higher than that of CSD. From ductility point of view, wall strengthened with PET-FRP behaves in a more ductile manner than CFRP strengthened wall as no rupture of FRP was observed in PSD walls. Moreover, unlike CSD, for the case of PET-FRP strengthened walls, the load did not drop much after reaching its full strength and a ductile mode of behavior can be seen in the post peak regime. In comparison with URM walls, both CSD and PSD walls have as much as twice the shear strength than URM walls. On the other hand PSD walls show similar ductile nature of URM walls but CSD walls are quite brittle and had lesser shear deformation at peak load than URM walls.

Wall strengthened by FRP grid system (CSG, PSG)

These walls were strengthened with FRP strips of 70 mm width each in a grid system as shown in Fig. 7(c) which covered approximately 40% of the gross wall surface.

In the case of the CFRP reinforced wall (CSG1), some fine-line diagonal cracks appear at the central area of the wall. It was not long after this, that more cracks appeared across the tension diagonal with simultaneous debonding of the CFRP strips, the load reached a level of 130 kN (Fig. 13). Almost simultaneously, one of the horizontal CFRP strips ruptured with a loud explosive sound, and the load dropped to 109 kN. With further displacement, the crack width increased and, in some places, the CFRP totally separated from the wall. Cracks of similar nature were observed on wall CSG2 as well, with the only exception is that the peak load was limited to 99 kN and no rupture of CFRP was noticed.

On the other hand, the walls PSG1 and PSG2, strengthened with PET-FRP, showed less stiffness than its counterpart, CFRP. For PSG1, at a load of about 120 kN, some debonding of the PET-FRP strip occurred along the tension diagonal. Almost simultaneously, a flexural crack followed by some discontinuous diagonal cracking appeared at the lower half of the wall on the heel side, and travelled all the way to the wall toe in a stepped fashion as shown in Fig. 13. With further displacement, the load remained almost constant but the wall slipped forward along the crack path and the experiment was terminated at that stage. Similar crack pattern was also observed in wall PSG2 as shown in Fig. 13 in a lesser degree and the peak load was limited to 88 kN. The comparison of lateral load-deformation response between PET-FRP and CFRP retrofitted walls is given in Fig. 12. Regarding ultimate load, both walls have similar shear capacities but PET-FRP behaves in a more ductile manner than CFRP. The mode of failure of those four walls look similar to each other and they are predominantly flexural cracking followed by diagonal shear slipping. Comparing with URM walls, both the two types of walls have shear capacity as much as three times higher than the URM walls. Walls when strengthening with PET-FRP grid system, the ductility is not compromised much in comparison with URM walls but for the case of CFRP strengthened wall ductility is reduced to almost half of the URM walls. It is also interesting to note that the ductility is not compromised substantially when the walls are strengthened with higher amount of FRP such as grid system than the amount of FRP in diagonal configuration. This phenomenon holds true for both PET-FRP and CFRP strengthened walls.

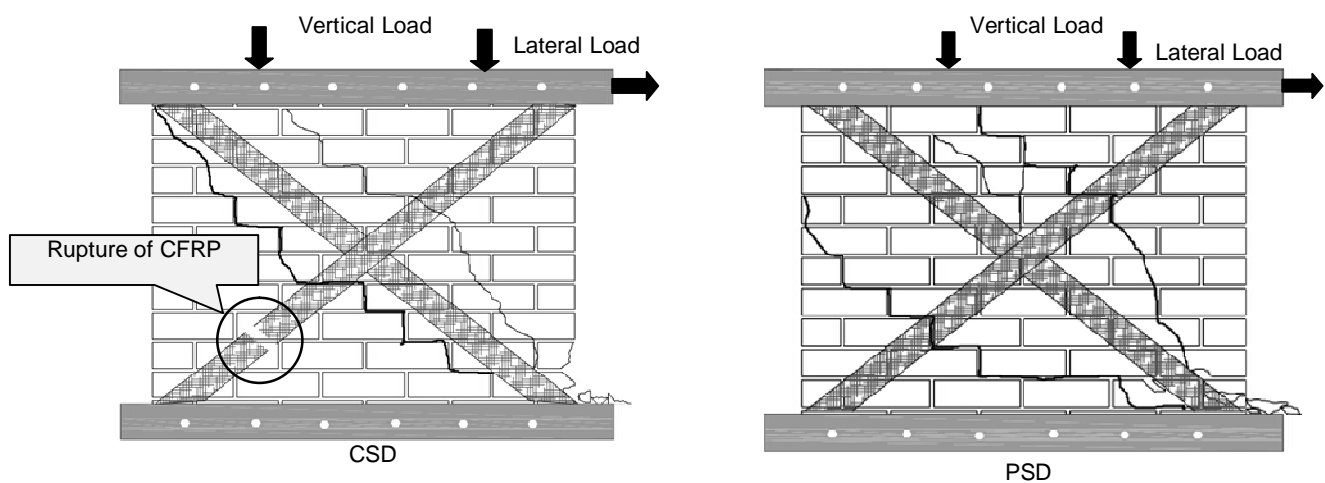


Figure 11. Schematic illustration of crack in diagonally FRP braced shear wall

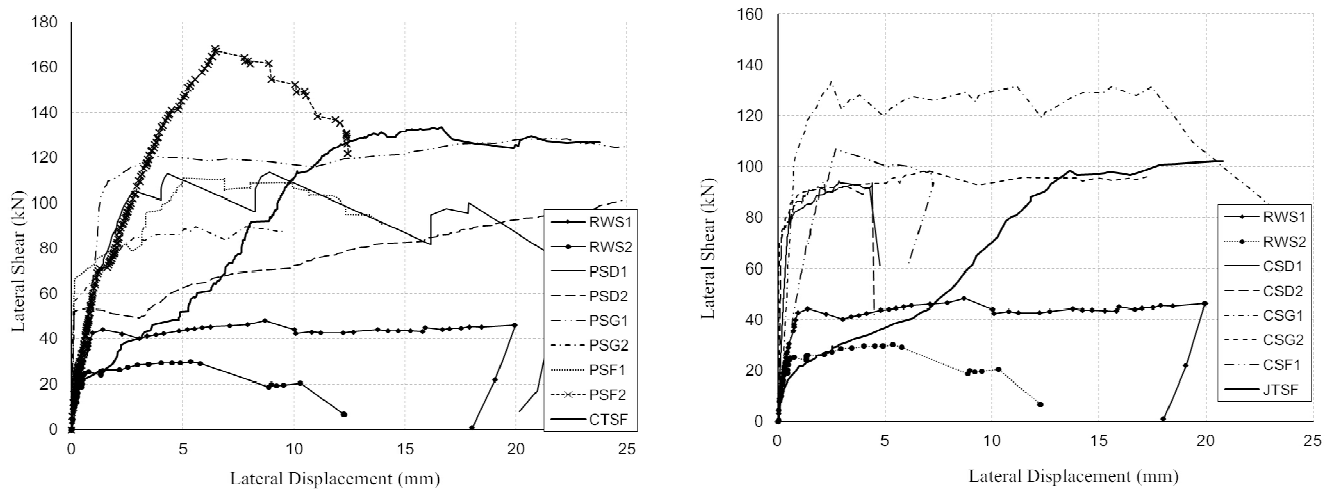


Figure 12. Load-deformation envelopes of all URM and FRP reinforced shear walls

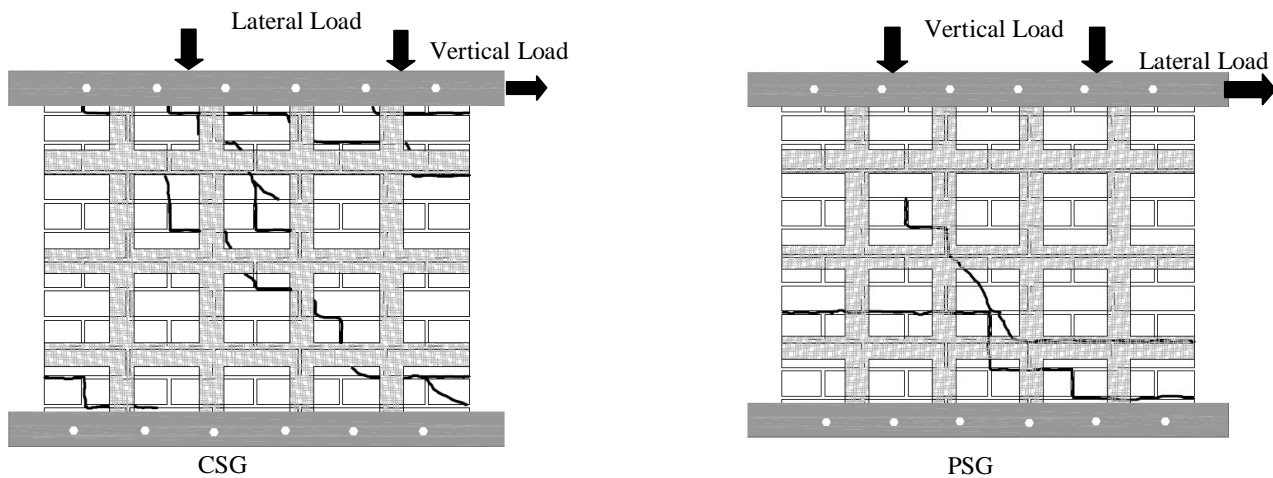


Figure 13. Schematic representation of crack in shear walls strengthened by FRP grid system

Fully wrapped walls (CSF, PSF)

These walls were strengthened by fully wrapping with FRP sheets according to Fig. 7(d). For CSF, the stiffness as well as the lateral load capacity was so high that the grip at the wall bottom prematurely failed before the wall attained its full strength. The wall PSF1 showed a high initial stiffness due to a higher percentage of PET, and remained unchanged until it reached about 60% of its peak shear capacity. Only after that, did the stiffness show a softening tendency, but no damage or crack whatsoever was seen on the wall, as the wall was fully covered by the PET-FRP sheets. Once it reached its full strength, further displacement only resulted in load reduction. It was observed that the wall was coming out from the grips at the bottom. The experiment was terminated at that point because it was impossible to continue as both the wall and jack were out of plane. For PSF2, similar phenomenon was happened at a load of 50 kN and the load raised to 160 kN. For wall strengthened by JUTE-FRP, a ductile load-deformation behavior can be seen in Fig. 12 with an ultimate load of 104 kN (see Table 1). On the other hand wall reinforced by COTTON-FRP (see Fig. 14) also show more ductile behavior than its counterpart CFRP or PET-FRP wall. Since all these walls were fully wrapped by the FRP sheets, damage, if any, could hardly be detected by visual observation.

It was quite clear from fully wrapped wall that higher the percent of FRP higher is the stiffness as well as shear strength of masonry wall. However, higher amount of FRP materials do compromise with the ductility of the wall and are not fitting well with the purpose of seismic strengthening.



Figure 14. Experimental setup of COTTON-FRP reinforced shear wall



Figure 15. Experimental setup of tension test of JUTE sheet

4 CONCLUSIONS & RECOMMENDATIONS

In this experimental study, fifteen masonry panels were tested, having been strengthened by two type of artificial and comparatively expensive FRPs such as CFRP, PET-FRP sheets and two types of naturally available but relatively cheaper FRPs such as JUTE-FRP and COTTON-FRP, in three different configurations with similar boundary conditions. Vertical loads were applied at two points prior to lateral loading. The rotation of the top beam was partially restrained by these two vertical loads. Load-deflection characteristics were observed for each wall and subsequent damages were evaluated. Simple analytical models are proposed for unreinforced masonry (URM) as well as FRP strengthened masonry walls. Based on the foregoing results and observations, the following conclusions can be drawn:

- i. The URM reference walls failed in shear sliding preceded by a flexural cracking, which is largely seen as premature failure of the URM wall. For FRP strengthened masonry walls, the failure mode changes to predominantly a diagonal tension, toe crushing, debonding and rupturing of FRP, or a combination thereof.
- ii. This experimental study demonstrates the ability of all of the FRPs such as CFRP, PET-FRP, JUTE-FRP and COTTON-FRP sheets to enhance the shear resistance to a great extent; more than twice the capacity of the URM wall. Among the four, PET-FRP has a better seismic performance than CFRP, as it shows a better ductile behavior than CFRP, especially in the post-peak region where there is a structural demand for integrity and margin of safety against collapse. Though the CFRP increases the shear capacity of a masonry wall, it substantially reduces the ductility of the wall, which may eventually cause an explosive type of masonry failure. On the other hand JUTE-FRP and COTTON-FRP also enhanced the shear capacity of masonry wall to almost twice of that of URM walls, but they show better ductility than CFRP or PET-FRP.
- iii. As masonry is quite fragile against lateral movement with a low lateral stiffness, diagonal bracing with PET-FRP sheet can be the one of the options if the cost of the material are not compromised, but seeking for a low-cost strengthening material, JUTE-FRP and COTTON-FRP could be the best option, where not only capacity enhanced but, at the same time, the wall is made quite ductile, substituting a ductile mode of failure for a catastrophic one. Moreover, unlike CFRP and PET-FRP, JUTE and COTTON are bio-degradable materials, that do not pose any threat to the ambient environment.
- iv. In all strengthening work, cost of the material and installation is prime concern of both engineers and builders. The cross-diagonal configuration requires least PET-FRP materials, whose material cost is less than CFRP, with the minimum amount of installation work among all the cases considered, including walls strengthened by CFRP strips. Wall when fully covered by CFRP or PET-FRP is not a viable option for external strengthening, but they are quite good when JUTE or COTTON sheet are used.
- v. Research work, numerical modeling, model codes and provisions for RC structures strengthened by FRP have gone a long way in the last two decades, whereas, it is still far away from standard design practice and performance based seismic assessment of masonry. A concerted effort and a harmonized

approach are needed for masonry to meet that target. With the use of well-tested materials with reasonable cost, expert installation crews, and proper design guidelines, externally bonded FRPs can be a unique solution to many masonry structures for retrofitting and rehabilitation purposes. Analytical models and relevant formulation proposed in this study can be one step forward in achieving this goal.

ACKNOWLEDGMENTS

The authors sincerely acknowledge the financial assistance from CASR grant of KUET and from RONPAKU fellowship of JSPS to carry out this research. The authors are also thankful to Nittetsu-Sumikin Materials Co. Ltd. Japan and Maeda Kosen Ltd. Japan, for their support in providing necessary materials for CFRP and PET-FRP, respectively, that have been used in this experiment. Study can be one step forward in achieving this goal.

REFERENCES

- ACI 440. (2008). "Guide for the design and construction of externally bonded FRP systems for strengthening concrete structures." American Concrete Institute, Farmington Hills, MI 48331 U.S.A.
- ACI 530. (2002). "Building code requirements for masonry structures" ACI 530/ASCE 5/TMS 402.
- AC 125. (2010). "Acceptance criteria for concrete and reinforced and unreinforced masonry strengthening using eternally bonded fiber-reinforced polymer (FRP) composite systems." ICC Evaluation Service.
- ACI- 147. (1994). "Masonry in the Americas." ACI Special Publication 147.
- ATC 40 (1996). "Seismic evaluation and retrofit of concrete buildings." Applied Technology Council, Vol-1.
- Ali, Q., Badrashi, Y. I., Ahmad, N., Alam, B., Rehman, S., and Banori, F. A. S.(2012) " Experimental investigation on the characterization of solid clay brick masonry for lateral shear strength evaluation." *Int. J. of earth sciences and engr.* 5(4), 782 - 791.
- Andreas, U. (1996). "Failure criteria of masonry panels under in-plane loading." *J. Struct. Eng.*, 122(1), 37–46.
- Abrams, D. P. (2001). "Performance based engineering concepts for unreinforced masonry building structures." *Journal of Progress in Structural Engineering and Materials*, Wiley Interscience, 3(1), 48–56.
- Abrams, D. P. (2004). Seismic assessment and rehabilitation of unreinforced masonry buildings in the USA." *SÍSMICA 2004 - 6° Congresso Nacional de Sismologia e Engenharia Sísmica*.
- Albert, M. L., Elwi, A. E., and Cheng, J. J. R. (2001). "Strengthening of unreinforced masonry walls using FRPs" *J. Compos. Constr.*, 5(2), 76 – 84.
- Altin, S., Anil,O., Kara, M. E., and Kaya, M. (2007). "An experimental study on strengthening of masonry infilled RC frames using diagonal CFRP strips" *Elsevier J. of Composites. Part B: Engineering*.1-14.
- Al-Chaar, G. (2002). " Evaluating strength and stiffness of unreinforced masonry infill structures." ERDC/CERL TR-02-1 report, Engineer Research and Development Center, US Army Corps. of Engineers.
- Alcaino, P. and Santa-Maria, H. (2008), "Experimental Response of Externally Retrofitted Masonry Walls Subjected to Shear Loading" *J. Compos. Constr.*, 12(5), 489– 498.
- Akın, E., Özcebe, G., Canbay, E. and Binici, B. (2014). "A Numerical Study on CFRP Strengthening of Reinforced Concrete Frames with Masonry Infill Walls", *J. of Compos. Constr.*, 18(2), 04013034.
- Anthoine, A., Magonette, G., and Magenes, G. (1994). "Shear-compression testing and analysis of brick masonry walls." Duma G (ed) *Proc. of the 10th European conf. on earthquake eng.*, Vienna, Austria, A.A.Balkema, Rotterdam p 1657.